Quantum Mazes: Luminescent Labyrinthine Semiconductor Nanocrystals Having a Narrow Emission Spectrum

Silvia H. De Paoli Lacerda,* Jack F. Douglas,* Steven D. Hudson, Marc Roy, Jerainne M. Johnson, Matthew L. Becker, and Alamgir Karim

Polymers Division, National Institute of Standards and Technology, Gaithersburg, Maryland 20899

ABSTRACT We exploit the polytypism of group II–VI semiconductors and the long-range dipolar interactions typical of CdSe nanoparticle formation to modulate the geometrical structure and the optical emission properties of novel branched CdSe nanocrystals through shape-dependent quantum confinement effects. X-ray diffraction confirms that these materials incorporate crystalline domains of cubic zinc-blende and hexagonal wurtzite within a polycrystalline growth form whose geometry can be controlled by varying thermodynamic conditions. In particular, labyrinthine-shaped nanoparticles of tunable dimensions are reproducibly synthesized based on a heterogeneous reaction between cadmium acetate in a solution in hexadecylamine and trioctylphosphine with Se as a solid precursor at a relatively low temperature (110 °C). The resulting highly branched CdSe structures resemble labyrinthine patterns observed in magnetic fluids and superconductors films in magnetic fields, and in lipid films and other materials where strong dipolar interactions "direct" large-scale pattern formation. Surprisingly, these novel maze-like structures emit light within a *narrow bandwidth* (full-width at half-maximum $\approx$ 33–42 nm) of the visible spectrum (508 nm $< \lambda <$ 563 nm), so the regular dimensions of the core regions of these branched structures govern their emission characteristics rather than overall nanoparticle size. This property should make these materials attractive for applications where luminescent materials having tunable emission characteristics and a narrow emission frequency range are required, along with the insensitivity of the particles' luminescent properties to environmental conditions.

KEYWORDS: quantum dots · confinement · luminescence · labrynthine solidification patterns · exciton localization · CdSe · potential directed pattern formation

Colloidal semiconductor nanocrystals are luminescent nanoparticles having a discrete energy structure caused by exciton confinement, making these particles exhibit features similar to both atoms and colloidal particles. The variation of confinement in semiconductor nanostructures often provides a framework for testing new physical phenomena through the manipulation of the quantum aspect of these particles. In particular, modification of the electron and hole wave functions can be achieved by varying the shape or size of the nanocrystals,[1–4] so methods that allow for tuning the shape of these nanoparticles in a controlled way have significant interest. So far, this effort has led to the development of diverse nanostructures such as rods,[1,3] tetrapods,[5] prisms,[6] cubes,[7] trees,[3] and other regular shapes.[1,2,8,9] These architectures display new electronic and physical properties, providing attractive building blocks for optoelectronics and nanoelectronics applications.

The synthesis of branched nanostructures exploits the polytypism common in group II–VI semiconductors. Such materials can incorporate domains of cubic zinc-blende structure as well as a hexagonal wurtzite structure within a single nanoparticle. Using this property, dots, rods, tripods, and tetrapods of CdSe have been previously synthesized using a high-temperature pyrolysis of suitable precursors in coordinating solvents containing a mixture of trioctylphosphine oxide (TOPO) and alkylphosphonic acids.[5,9,10] The specific adsorption of surfactants to particular crystallographic planes alters the relative growth rates of different facets, providing a way of controlling the nanocrystal shape. The dipolar nature of the CdSe particles can also be expected to play a role in this complex crystallization process. Practical control over branching in this pattern formation process is achieved by adjusting the temperature to a range in which zinc-blende is preferentially formed during nucleation and where wurtzite growth occurs preferentially along the *c*-axis.[5] This method yields structures in which the arm length and number of branch points are controlled and uniform in their geometrical characteristics throughout the sample.[11]

Synthesis of more sophisticated nanostructures can be achieved by fine-tuning

*Address correspondence to silvia.lacerda@nist.gov; jack.douglas@nist.gov.

Received for review July 23, 2007 and accepted October 10, 2007.

Published online November 30, 2007.
10.1021/nn700111c

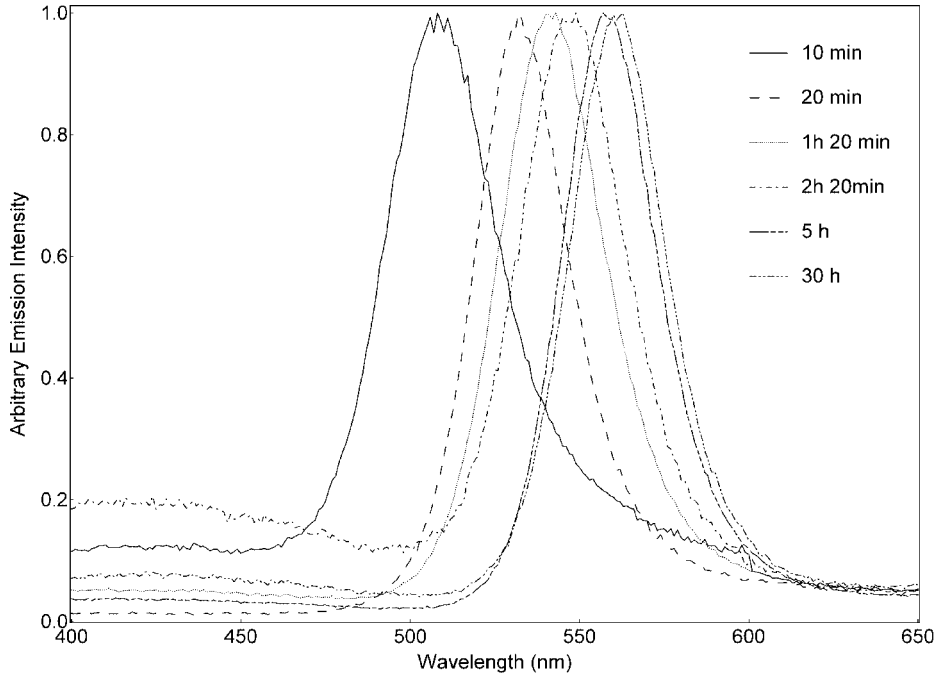

Figure 1. Tunable emission spectra of CdSe nanocrystals in toluene at room temperature after various reaction times (10 min, 20 min, 80 min, 140 min, 300 min, and 30 h). Excitation was performed at a wavelength of 350 nm.

the relative stability of wurtzite and zinc-blende structures of CdSe. The ultimate goal is switching the growth of these two phases on and off in a controlled way. To achieve this end, the kinetic and thermodynamic parameters governing the growth (temperature, solvent, and monomer concentration) must be carefully regulated.

In the present work, we form labyrinthine CdSe nanoparticles that luminesce in the visible optical frequency range by growing these nanocrystals at relatively low temperatures (as low as 110 °C) in the presence of trioctylphosphine (TOP) and hexadecylamine (HDA). This low-temperature synthesis favors the zinc-blende structure during nucleation, and under these conditions the TOP/HDA mixture *does not* preferentially stabilize a particular face of the crystal as in the "regularly" shaped quantum dot synthesis method mentioned above. This modification of the synthesis allows for the growth of open structures (see Figure 2) having arms with spacings apparently regulated by the long-range dipolar interactions characteristic of CdSe nanoparticles.[12] We find that the emission spectrum from these novel nanocrystals can be tuned by varying the arm configuration of these structures, while the luminescence lifetime is nearly constant. Transmission electron microscopy (TEM) images show that the morphology of the crystals resembles the labyrinthine patterns of ferrofluids and lipid films where dipolar interactions regulate the pattern formation[12–15] (see Discussion below).

Prior synthesis of CdSe nanocrystals utilized a protocol using dimethylcadmium (decomposition temperature ≈ 150°C), so that the nucleation took place near 180°C. Synthesis under these conditions yields quantum dots that emit in the yellow to red frequency range.[16,17] Following Peng and co-workers,[1] we utilized a "greener" reaction scheme, involving cadmium acetate (CdAc), which allows for selective nucleation and anisotropic growth at a relatively low temperature of 110 °C. This gives rise to complex-shaped luminescent nanostructures that are quite different from those obtained in the high-temperature synthesis with dimethylcadmium.

CdSe exists in both hexagonal wurtzite and cubic zinc-blende phases. The reported room-temperature band gap of wurtzite CdSe is 1.738 eV, and that of zinc-blende CdSe is 1.66 eV.[18,19] This energy difference between wurtzite and the zinc-blende structures is only a few millivolts per atom, so switching between the two growth modes can occur during the growth. Factors that affect the preference for cubic or hexagonal phase include temperature, concentration of precursors, and the presence of coordinating ligands.[20]

RESULTS

The 3D nanoparticles are hybrid structures of the two phases in which CdSe crystals can grow. The low reaction temperature favors the zinc-blende structure during the nucleation stage so that the core of the nanoparticles has a zinc-blende structure. Wurtzite arms then emanate from the f(111) faces of a zinc-blende core in a fashion similar to spherulite formation.[21] At a later stage, the zinc-blende structure nucleates again off the wurtzite arm, and the cycle is repeated. The key feature in this process is the manipulation of the kinetics and thermodynamics governing crystal growth. In the synthetic procedure described here, the thermodynamic growth favors both wurtzite and zinc-blende CdSe polycrystalline structures, yielding sophisticated light-emitting nanostructures.

The influence of quantum confinement on the electronic and optical properties of semiconductor nanocrystals is especially interesting technologically for direct bandgap II–VI semiconductors such as CdSe and CdTe. Increasing control over the size, shape, and surface chemistry has enabled the production of quantum dots, rods, and pods of these materials with tunable (from blue to red) narrow-band luminescence and high

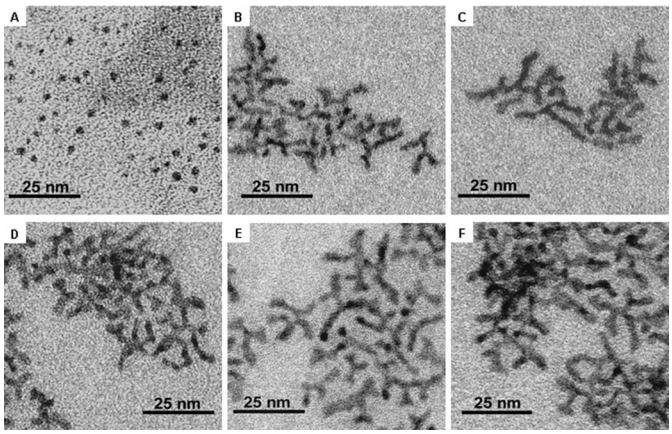

Figure 2. Transmission electron microscopy images of CdSe branched nanostructures sampled at different reaction times: (A) 10 min, (B) 20 min, (C) 80 min, (D) 140 min, (E) 300 min, and (F) 30 h.

quantum yields[11,17,22] and with optical properties directly dependent on particle shape. Based on this phenomenon, the growth kinetics of semiconductor nanoparticles can be monitored by the temporal evolution of the emission spectrum as shown in Figure 1.

When the temperature reached 110 °C, the colorless initial solution became green-yellow, and the first fraction was collected for analysis (image A in Figure 2). Quantum dots with dimension of 2.3 nm ± 0.3 nm (uncertainty determination is described in the Methods section) with a narrow emission profile were then obtained. Initiation of growth with zinc-blende dots is a prerequisite for the synthesis of these branched structures.[20,23,24] The initially synthesized zinc-blende quantum dots evolve into thick-armed branched structures as the reaction progresses, and there is an accompanying color change from yellow to red-brown luminescence. The arms bend to avoid each other without collision and repeatedly branch.

The optical properties of the branched nanostructures correlate with changes in the diameter of the rods making up the arms, which slowly change from 2.3 nm ± 0.3 nm to 3.6 nm ± 0.4 nm during a 30 h growth period. This arm growth is nearly linear in time and corresponds to a progressive red shift in the emission spectrum wavelength, λ_e, of the particles from 508 to 563 nm. At long times, λ_e stabilizes at nearly 563 nm. Despite the geometrical irregularity of these nanocrystals, they exhibit a narrow emission peak bandwidth (33–42 nm), similar to that of relatively monodisperse spherical CdSe quantum dots. The nanoparticle growth parameters and the luminescence properties of our CdSe particles are summarized in Table 1. The tunability of the photoluminescence (PL) emission is attributed to the increase in arm diameter, as previously established for straight quantum wires[25] and tetrapods.[26]

That the zinc-blende/wurtzite polytypism occurs throughout the reaction was confirmed by X-ray diffraction (XRD, Figure 3). The diffractograms exhibit three major peaks, which are broadened, an effect arising mainly from the small size of the crystals but also from the superposition of multiple reflections. The first of these peaks is found at 25°; this comprises the (111) zinc-blende reflection and the (100), (200), and (101) wurtzite reflections. The second peak, at 42°, comprises the (220) zinc-blende and the (110) wurtzite reflections. The third peak, at 50°, comprises the (311) zinc-blende and the (112) wurtzite reflections. From these peaks alone, it is not possible to evaluate whether the nanocrystals are one crystal type or another. From samples both early and late in the reaction process, an additional contribution to the diffracted intensity is observed, however, at 46° (see insets, Figure 3). This contribution arises solely from the (103) wurtzite reflection, and zinc-blende has no corresponding reflection. While in pure wurtzite the (103) reflection has intensity comparable to that of the others [*i.e.*, (002), (110), and (112)],[9,10,20] a diminished intensity here indicates that zinc-blende is also present. An inherently weaker reflection also associated only with wurtzite is the (102) reflection observed at 35°. Therefore, both wurtzite and zinc-blende structures coexist in these nanocrystals, throughout their growth process, and these branched nanoparticles are polycrystalline in nature.

Time-resolved spectroscopy is a powerful technique to probe energy relaxation and recombination dynamics in quantum nanostructures. The shape evolution dependence on the lifetime decay of CdSe is demonstrated in Figure 4, which shows decay curves for

TABLE 1. Recovered Time Constants from the Double-Exponential Decay Fits of the Time-Resolved Fluorescence Signal of the CdSe Nanocrystals at Different Reaction Times

reaction time	peak emission (nm)	$\tau_{PL\,1}$ (ns)	$\tau_{PL\,2}$ (ns)	a_1 (%)[a]	a_2 (%)[a]	arm diameter (nm)
10 min	508	1.6 ± 0.2	6.6 ± 0.6	79	21	2.3 ± 0.3
20 min	532	1.3 ± 0.3	5.8 ± 0.4	74	26	2.7 ± 0.3
1 h 20 min	543	1.3 ± 0.3	5.8 ± 0.4	75	25	3.1 ± 0.3
2 h 20 min	549	1.3 ± 0.3	5.8 ± 0.4	75	25	3.3 ± 0.3
5 h	557	1.2 ± 0.3	5.7 ± 0.4	74	26	3.4 ± 0.5
30 h	563	1.2 ± 0.3	5.6 ± 0.4	73	27	3.6 ± 0.4

[a] a_1 and a_2 are population factors.

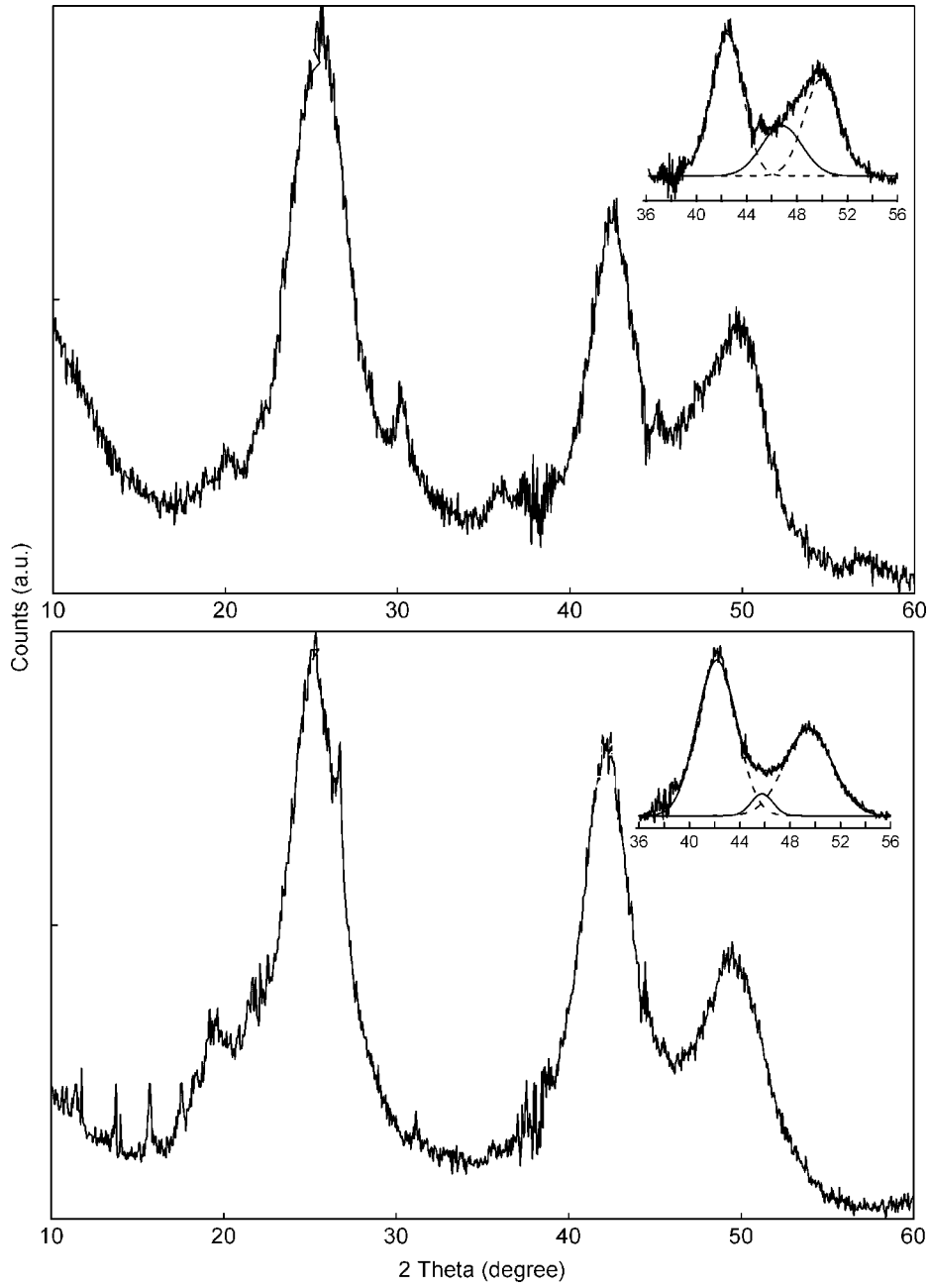

Figure 3. X-ray diffraction patterns of CdSe nanocrystals formed at (top) 10 min and (bottom) 30 h. Insets: Deconvoluted curves showing the presence of the (103) wurtzite reflection at $2\theta \approx 46°$.

some selected samples grown at 110 °C (10 min and 30 h). The typical PL decay spectrum consists of two time-decay components, each having a time constant on the order of nanoseconds. The faster-decaying component (emission from a spin-allowed singlet exciton state) is dominant over the slower one (emission from a spin-forbidden triplet state), and both are constant for all the nanostructures obtained after 20 min of reaction, indicating that *the transition probabilities do not change with changes in nanoparticle shape, within experimental uncertainty*. Table 1 contains lifetime and population values for samples collected at 10 min, 20 min, 1 h 20 min, 2 h 20 min, 5 h, and 30 h. For the early growth sample collected at 10 min, the PL lifetime values, τ_{PL}, are higher (6.6 and 1.6 ns) than those of samples collected later, whose τ_{PL} are essentially constant throughout the growth process (τ_{PL} averages from 20 min to 30 h reaction times are 5.7 and 1.3 ns, respectively). These τ_{PL} estimates are in qualitative consistency with values reported by Lee *et al.*,[27] which ranged between 1 and 6.3 ns. The slight decrease in τ_{PL} for the late stage of crystal growth is attributed to the creation of a new path for depopulating the excited state, which indicates a transformation of the electronic structure of the nanocrystals as the reaction proceeds. Previous measurements on spherical quantum dots have shown that the τ_{PL} decreases with the increasing size of quantum dots.[28] However, de Mello Donega *et al.*[29] also em-

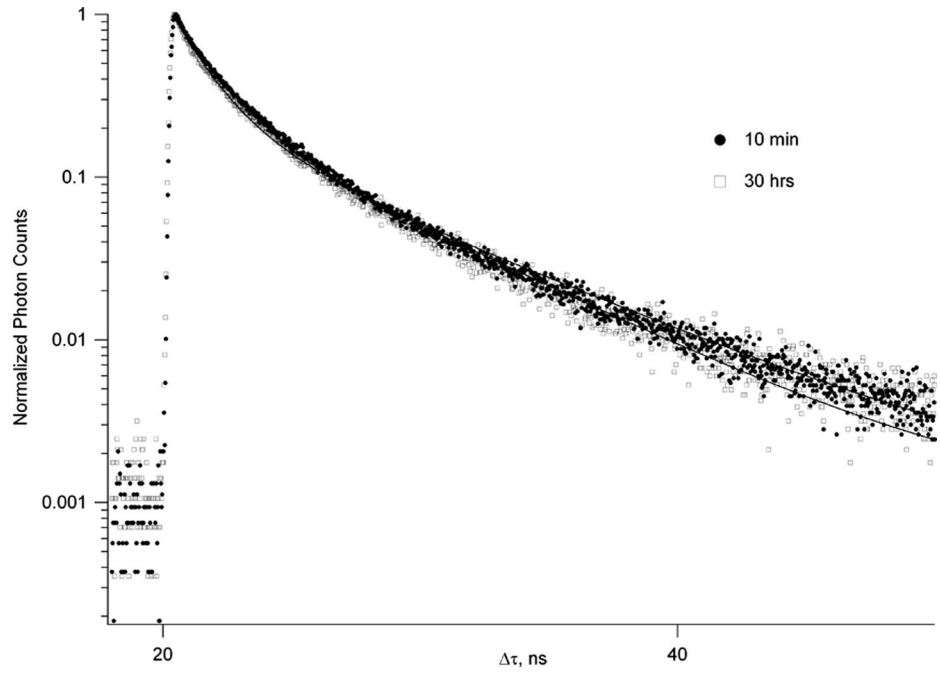

Figure 4. Time-correlated single photon counting fluorescence signal of CdSe nanocrystals formed at 10 min and (●) and 30 h (□), where the observations correspond to a wavelength of 570 nm. Lines indicate a fit to a double-exponential function.

ployed a relatively low synthesis temperature (170 °C), and they also found a correlation between growth geometry and the luminescence properties of CdSe quantum dots that is reminiscent of our own observations. Specifically, they found a rapid increase τ_{PL} after the initial 10 min reaction time and then found that τ_{PL} stabilized to a lower value after 30 min. Also, τ_{PL} did not change at later times as the crystals kept growing. Although the origin of these changes in τ_{PL} in these CdSe nanostructures with reaction conditions is not currently clear, our working model of this phenomenon is that the fast decay component roughly arises from transitions between electronic bands, while the slow decay component reflects a trapping of surface-localized electronic states.[28,30]

Since the unusual particle morphology in our quantum dot material clearly has a large impact on the optical properties of these materials, we consider the basic mechanism of this growth process. First, the growth of elongated nanocrystals requires a high chemical potential environment, *i.e.*, high monomer concentrations. This thermodynamic condition has a strong impact on the nucleation process. Using a Cd-to-Se millimolar concentration ratio of 1.47:1, we obtained quantum dots that evolved into branched structures (see Figure 2) for about 30 h, and after that time the reactants were consumed and growth attenuated. Upon increasing the concentration of Se (Se:Cd millilmolar concentration ratio equals 2:0.47), the reaction rate increased, and in this case only spherical quantum dots were formed (data not shown). Se is more reactive than Cd, and this leads to a faster nucleation process and a greater number of initial nuclei. The nucleation process consumes the monomers to a point that further growth of the quantum dots into branched structures does not occur. Evidently, the initial nucleation kinetics play a primary role in determining the final morphology of our nanoparticles.

Selective binding of ligand surfactants on the surface of nanocrystals has been suggested to control the shape of nanocrystals.[9,31,32] However, this binding phenomenon should not be as important in the initial stage of crystallization as the concentration of monomers is for binding. In many studies, TOPO is chosen as the ligand surfactant and has been found to induce the growth of spherical quantum dots. The addition of tetradecylphosphonic acid (TDPA) decreases the reactivity of Cd, slowing the reaction while stabilizing the wurtzite structure, and enabling the formation of rod-like morphologies.[10] Previous syntheses of these nanoparticles using this chemistry were performed at relatively high temperatures ($T > 200$ °C). We studied the effect of TOPO and TDPA on the kinetics of growth and the shape of CdSe nanocrystals using our low-temperature procedure. Synthesis was carried out at the same Cd:Se ratio (1.47:1 mmol) and TOP concentration (15.7 mmol). The concentration of HDA was decreased by half (10.71 mmol), and TOPO or TDPA was added (10 mmol) such that the total ligand concentration was the same in all the reactions. It was found that, by adding TOPO, the reaction was slowed slightly, which led to the formation of similar red-emitting branched crystals reaching their final size after 24 h with arms of 3.5 nm ± 0.6 nm dimensions, similar to those obtained by reaction without TOPO (3.6 nm ± 0.4 nm). TDPA addition also slowed the reaction slightly, but high-quality pure zinc-blende

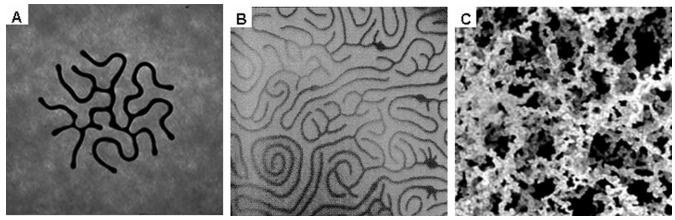

Figure 5. Labyrinth growth patterns. (A) Patterns observed in a 100 mL ferrofluid droplet confined within a 1.1-mm-gap Hele–Shaw cell with a 155 G magnetic field applied in a direction orthogonal to the film plane.[15] [Image provided by Dr. Markus Zhan, Laboratory for Electromagnetic and Electronic Systems, Massachusetts Institute of Technology.] (B) Pattern formation in a langmuir film of phospholipids whose polar groups endow them with a permanent (or induced) electric dipole moment. [Reprinted with permission from ref 34. Copyright 1995 American Association for the Advancement of Science (http://aaas.org).] (C) Polycrystalline coral-like structures formed through the self-organization of dipolar Ni particles.[68] Morphologically similar (fluorescent) "coral-like" patterns have been observed in porous acid-etched silicon,[54] although the spatial resolution of these earlier measurements was more limited. Note that the nanoparticles retain their integrity in this image.

quantum dots with size tunable from 1.9 nm ± 0.2 nm to 4.3 nm ± 0.4 nm and a narrow emission profile were obtained instead of branched nanoparticles (data not shown). These results indicate that the effect of different ligands on the architecture of the CdSe nanocrystals is temperature dependent. The CdSe nanocrystal architecture is thus sensitive to the choice of ligand, ligand concentration, and temperature, so a considerable amount of thermodynamic control on the growth morphology can be exerted by regulating the reaction conditions.

DISCUSSION

Origin of Labyrinthine Growth Patterns. The general tendency of these growth patterns to adopt the labyrinthine patterns shown in Figure 2 deserves comment. Such patterns are characteristic of numerous nonequilibrium growth processes involving particles having magnetic, electrical, or other interactions of a dipolar form.[33] The CdSe particles are known to exhibit a large permanent dipolar moment[34,35] (typically in the range of 50–100 D; 1 D = 3.336×10^{-30} Coulomb · m), so the pattern of behavior observed in Figure 2 should perhaps not be surprising.

This generic instability is thought to be due to two main competing effects.[33] The arms are nucleated and grow outward from the initial seed that sets the original growth symmetry. Under highly nonequilibrium growth conditions, there is also a tendency for arm fission. This arm-splitting process is also found in ordinary dendritic crystallization (*i.e.*, the Mullins–Sekerka instability),[36,37] as well as in the mathematically related problem of the unstable interface created by injecting a fluid into a more viscous fluid (Hele–Shaw instability).[37,38] The long-range dipolar interactions apparently ensure that the "dendrite" arms in these far-from-equilibrium growth forms adopt energetically respectful distances from each other, resulting in branched structures with a relatively uniform distance between the arms, reminiscent of the famous Peano and Hilbert curves of classical analysis[39] (see Figures 2 and 5). A geometrically similar type of potential directed pattern formation occurs in reaction diffusion fronts, where the antagonistic repulsive interactions and the outward growing nature of the growth pattern can lead to uniformly space-filling growth patterns.[40,41] Patterns of this general type have been extensively investigated in the context of ferrofluids subject to magnetic fields,[12,42,43] superconducting materials in magnetic fields,[44] Langmuir monolayers of polar lipid molecules,[45,46] and thin garnet films,[47,48] and even the organization of living cells.[49] For comparison, we illustrate labyrinthine ferrofluid and Langmuir monolayer patterns in Figure 5A,B. Although coral-like labyrinthine patterns (see Figure 5C) having a strong and narrow fluorescence emission spectrum have been observed in porous electrochemically etched silicon acid,[50] the growth patterns shown in Figure 2 provide the first documented example of this type of pattern formation where *discrete particles* form rather than a macroscopic network structure.

Some features of the labyrinthine growth process are not captured by the explanation above. The structures shown in Figure 2 probably involve an oscillation between zinc-blende and wurtzite structures, so these growth forms also have some resemblance to spherulite growth where new grains branch off from the growth front.[51] These complications will require a more elaborate analysis than former analyses of this type of branched growth form to account for this type of secondary nucleation phenomenon, and further experimental studies are required to better understand the main physical parameters that serve to regulate the geometrical properties of these rather unique growth forms.

Optical Properties of Branched Nanoparticles. Apart from the manner in which these particles grow, our observations on the optical properties of these materials raise interesting questions about the effect of geometrical disorder on quantum confinement in semiconductor materials. Previous studies have repeatedly indicated that size polydispersity of quantum dots and quantum wires tends to greatly broaden the emission spectra of the quantum particles,[52,53] yet we do not see such an effect in our labyrinthine growth structures. Behavior of this kind has been observed before in the fluorescence emission spectra of porous electrochemically etched silicon, where highly branched "coral-like" structures having arm diameters of less than 5 nm were found to be associated with these strongly fluorescent materials.[54] Cullis and Canhan[54] made the interesting suggestion that the high quantum efficiency and strong fluorescent emission of this class of materials can arise from the enhanced exciton localization caused by the bending and branching of the labyrinthine nanowire silicon

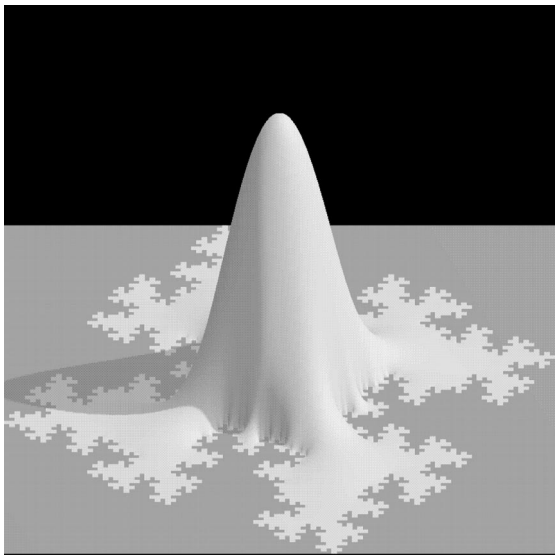

Figure 6. Fundamental vibrational mode of a model drum with a rough boundary. This solution of the Helmholtz equation is also the ground-state stationary solution to the Schrödinger equation with a repulsive wall (Dirichlet) boundary condition, and the relation between these problems is described by Sapoval *et al.*[58]

network and that this irregular geometry, in turn, was responsible for the high emission efficiency. Since this early work, there has been much evidence confirming aspects of this intuitive argument that the disordered nature of these networks might confer adsorption characteristics superior or at least comparable to those of more perfect nanoparticles. Hasen *et al.*[50] showed how the introduction of discrete junctions between quantum wires can cause the emission spectra of the isolated wires to make a "striking transition" from broad and continuous photoluminescence into energetically sharp and spatially localized emissions at low temperatures for quantum wires forming a T-junction. The formation of highly localized states at well junctions has also been reported in several recent measurements,[55–57] and there seems to be no doubt about the existence of this effect. From a theoretical standpoint, this tendency toward the formation of strongly localized excitonic states in branched structures can be understood to arise from a general tendency of waveforms (acoustic as well as quantum mechanical) to become localized near the central nodal regions from which the branches emerge.[58–61] This "screening" effect makes the quantum mechanical wavefunction ψ for the excitons localized, and thus ψ in the branch node region is large in amplitude. Outside this region, ψ decays rapidly to zero, so such branched nanoparticles should appear to be much larger than the spectroscopically determined confinement dimension. To illustrate this effect graphically, we show in Figure 6 the fundamental vibrational mode of an idealized clamped drum (or equivalently the ground-state wavefunction) with a central regular-shaped region surrounded by an irregular boundary, as in the shapes of our nanoparticles. We see that the drum deformation (quantum mechanical wavefunction) amplitude is evidently localized to the central region away from the rough boundary, where the deformation (wavefunction) essentially vanishes. The formation of a localized state of this type is strongly indicated in our labyrinthine quantum particles, as evidenced by the narrow emission bandwidth that resembles those of solutions of monodisperse spherical quantum dots. It has also been predicted from simple particle-in-a-box calculations[62] similar to those indicated in Figure 6 that these strongly localized (excitonic) quantum states in the core region of the nanoparticles should exhibit a *weak coupling* to excited electronic states localized on the particle surface due to the low wavefunction amplitude of the particle core-localized states and thus a low overlap of the wavefunctions describing the core- and surface-localized electronic states.[58] Thus, wavefunction "screening", arising for structural irregularity away from the branching nodes of the nanoparticles, is expected to also inhibit excitation–recombination processes at the periphery of the particles and thus should enhance the average fluorescence lifetime.[58] Consistent with this interpretation, Salman *et al.*,[63] Pang *et al.*,[64] and Wang *et al.*[65] found that the tetrapods have absorption features similar to those of dots and suggested that this could be understood in terms of lowest localized exciton electronic states at the core of these structures. We then have an attractive general explanation of how high luminescence yield, strong photoluminescence, and relatively narrow adsorption and emission spectra can be consistent with nanoparticles having appreciable structural heterogeneity.

Recent measurements on regularly branched (tetrapod) quantum particles, however, suggest that factors other than wavefunction localization at branching nodes must be important in some nanoparticles. In particular, although the fluorescence properties of these branched nanoparticles show optical absorption characteristics consistent with the formation of localized states in the particle core regions,[24,66] the tetrapods can apparently exhibit a strong coupling between the nanoparticle core regions and excited states localized in the nanoparticle arms, an effect that can appreciably enhance radiative recombination. Factors influencing the extent of coupling between the core and peripheral regions of branched nanoparticles are evidently important for understanding the electronic properties of these complex-shaped particles. This observation leads us to consider the possibility that the polycrystalline nature of the nanoparticles could have a crucial effect on their optical properties.

Potential Grain Boundary Effects. Since the grain structure of our branched nanoparticles is evidently of potential relevance to an understanding of these particles, it is useful to compare the labyrinthine nanoparticles to polycrystalline nanowires formed by removing the

ligands from the surface of spherical quantum dot in solution. Upon removing the ligands, the dipolar interactions of the (CdTe) quantum dots predominate the interparticle interactions,[67] and long "pearl-like" necklaces of quantum dots self-assemble in solution and then slowly fuse (recrystallize) to form quantum wires. This two-step process of particle formation and accretion appears to be a rather common mode of nanoparticle organization, and Zhang *et al.*[68] have examined the formation of coral-like polycrystalline growth forms in dipolar Ni particles (see Figure 5C). Porous, electrochemically etched silicon exhibits a strikingly similar morphology, as well as a strong and narrow fluorescence emission spectrum,[54] as in the case of our CdSe nanoparticles.

"Strings" of CdSe dots have been observed to be highly luminescent relative to other direct bandgap semiconductor particles with large aspect ratios (>10). Indeed, the fluorescence quantum yields of these "composite" particles were claimed to be as high as 29% for green nanowires investigated by Tang *et al.*[67] It is probably correct to view the nanoparticles in these strings as separated by grain boundaries, which is also a reasonable model of our branched nanoparticles. On the basis of these observations, we suggest that the grain boundary structure of a polycrystalline aggregate of nanoparticles might serve to enhance exciton localization and, thus, enhance the adsorption and fluorescence intensities of these polycrystalline materials. It seems that such a picture also applies to porous silicon materials, where a string of ball-like nanocrystallites has been suggested to underlie the strong, narrow-wavelength, and tunable photoluminescence of these materials.[54,69] Fluctuations in the thickness of quantum wires has also been roughly described in terms of a string of quantum dots that are decoupled somewhat by surface undulations of the wire surface.[50] We expect that the formation of interfaces within polycrystalline nanoparticles will create a more effective decoupling between regions within the nanoparticles than surface undulations in near single-domain crystalline structures.

The manner in which our particles form labyrinthine patterns must also be important for understanding the luminescence properties of these particles. Evidently, a regular labyrinthine spacing is required to have a narrow emission spectrum, as in individual and strings of particles having a highly uniform size. We mentioned before that a narrow absorption spectrum is found for straight rods,[25] and it has been found that this adsorption spectrum broadens appreciably if there is an appreciable polydispersity in the diameter or length of these structures.[66,70] It seems to be crucial that the separation of the particle arms is sufficiently large to let these particles exhibit the quantum effects that make them desirable from an application standpoint. Crystallization of the CdSe nanoparticles can lose the fluorescent properties because of strong interparticle interactions.[28] The labyrinthine pattern apparently allows for the largest mass density of CdSe material possible, while still preserving the fluorescent optical properties of this type of particle. These structures evidently raise many interesting questions about which geometrical forms of the quantum particles are optimal for particular applications and about how disorder affects the optical properties of these materials.

CONCLUSIONS

We have synthesized and characterized novel branched CdSe nanocrystals grown under relatively low temperature reaction conditions. The resulting highly branched CdSe structures resemble labyrinthine patterns observed in magnetic fluids and lipid films, where strong dipolar interactions "direct" the large-scale pattern formation. The nanocrystals exhibit a high degree of solubility and stability in toluene and provide novel building blocks for nanotechnology applications. The growth mechanism of these nanoparticles is consistent with an initial nucleation of zinc-blende quantum dots, followed by the growth of arms from a wurtzite particle. Despite the irregular appearance of these labyrinthine particles, they emit light within a *narrow* bandwidth of the visible spectrum. Evidently, the regular dimensions of the core structure of these branched particles dominate their emission characteristics rather than overall particle shape, since the ground-state excitonic wavefunction are mostly confined in the nanoparticle core region.[58] Moreover, we suggest, following ref 59, that the irregular shape of these particles can actually enhance the fluorecence lifetime by weakening the coupling between electronic states in the core of the nanoparticle and the surface-localized excited electronic states so that the branched structure surrounding the core of these nanoparticles serves to effectively isolate these particles from their environment. This property should make these materials attractive for applications where luminescent materials having a tunable and narrow emission frequency range are required and where an insensitivity of these properties to environmental conditions is desired.

METHODS

Cadmium acetate (CdAc, 99%), selenium (Se, 99.9%), trioctylphosphine (TOP, 99%), and hexadecylamine (HDA, 98%) were used as received from Aldrich. Trioctylphosphine oxide (TOPO, 99%) and tetradecylphosphonic acid (TDPA, 99%) were obtained from Alfa. Anhydrous methanol, toluene, and chloroform were purchased from Aldrich and used without further purification.

Synthesis of CdSe Nanocrystals with Labyrinthine Morphology. In typical synthesis of CdSe nanocrystals, a mixture of 5 g of HDA (20.71

mmol), 7 mL of TOP (15.7 mmol), and 0.392 g of CdAc (1.47 mmol) was heated at 180 °C for 1 h under an argon atmosphere. Next, the temperature was decreased to 60 °C, and 0.079 g of Se (1 mmol) powder was added to the reaction flask. The temperature was raised slowly to 110 °C. The color of the solution changed from light yellow to red. Alternatively, labyrinthine CdSe nanocrystals were prepared by adding 10.71 mmol of HDA and 10 mmol of TOPO. Samples were purified by precipitation of the nanocrystals with methanol and subsequent dispersion in chloroform.

Synthesis of Zinc-Blende CdSe Quantum Dots. Pure and high-quality zinc-blende CdSe quantum dots can be synthesized using the same low-temperature heterogeneous reaction by adding 10 mmol of TDPA and decreasing the concentration of HDA to 10.71 mmol.

Sample Characterization. The crystal structure of the nanocrystals was characterized by X-ray diffraction, using a 0.154 nm Cu Kα Ni-filtered source. Diffractograms were recorded from purified and precipitated powder using a Rigaku[72] reflectometer operated in reflectance mode at 1600 W, with an exit angle 2° and entrance slits. A 2θ diffraction angle was scanned from 10° to 70° in steps of 0.05°, with an acquisition time at each step equal to 3 s. Since some diffraction from the underlying aluminum sample holder was observed, a diffractogram of the empty holder was also recorded and subtracted from the sample diffractogram.

The structure, size, and shape of the nanocrystals were measured by transmission electron microscopy performed on a Philips EM 400T microscope operating at 120 kV equipped with a Soft Imaging System CCD camera (Cantega 2K). TEM samples were prepared by dropping diluted solutions of quantum dendrons in chloroform or toluene onto 600-mesh carbon-coated copper grids. Particle size is an average of 20–30 individual particle sizes, and the uncertainty is the standard deviation of the size distribution. Luminescence emission profiles were obtained on a Cary Eclipse fluorescence spectrophotometer.

Time-Resolved Fluorescence Measurements. The time-resolved fluorescence signals were collected by a custom-built time-correlated single photon counting (TCSPC) apparatus using a Becker and Hickl SPC 830 module. The vertically polarized 465 nm excitation light was obtained from a supercontinuum by passing it through a monochromator (Instrument SA Inc. H-20[72]). The monochromator, with a slit width of 1 mm, has grating rulings of 1200 grooves/mm, a 0.5 nm resolution, and a band pass of 4 nm. The continuum was generated as 20 nJ pulses of 790 nm light from a 2 MHz cavity-dumped Ti–sapphire oscillator laser system (Kapteyn-Murnane Laboratories Inc. Cascade) that were propagated through a 12 cm length photonic crystal fiber (Crystle Fiber). The fluorescence emission was detected at magic angle (54.7°) by a PMC-100 fast detector (Becker and Hickl), with a typical rise time of 150 ps. The emission wavelength range detected was selected with a band-pass filter centered at 570 nm ± 20 nm. The resulting instrument response function was Gaussian shaped with a full-width at half-maximum (fwhm) of 200 ps. The TCSPC setup was calibrated with the known fluorescence standard Rhodamine 6G in methanol. The measured fluorescence lifetime of the dye is 4.1 ns ± 0.2 ns, which is in good agreement with the 4.16 ns time constants reported in the literature.[71] Sample mixtures were contained in a quartz cuvette cell, with path length of 1 cm. The error for each fit was determined by using the standard error analysis method described by the equation

$$\sigma_i = \sqrt{C_{ii}\chi^2} \quad (1)$$

where C_{ii} is the diagonal element of the variance–covariance matrix and χ is reduced chi. The reduced χ^2 value for each fit was determined to be between 0.00002 and 0.00003, with root-mean-squared values R between 0.99731 and 0.99791.

Acknowledgment. We are grateful to Dr. Markus Zhan of the Laboratory for Electromagnetic and Electronic Systems, Massachusetts Institute of Technology, for providing the image of pattern formation in a ferrofluid in an applied magnetic field (Figure 5A) and Bernard Sapoval of the Laboratoire de Physique de la Matière Condensée, Ecole Polytechnique, for providing us with an image of the solution to the wave equation with a rough boundary (Figure 6).

REFERENCES AND NOTES

1. (a) Peng, Z. A.; Peng, X. Synthesis of High Quality Cadmium Chalcogenides Semiconductor Nanocrystals Using CdO as Precursor. *J. Am. Chem. Soc.* **2001**, *123*, 183. (b) Peng, X. Mechanisms of Shape Control and Shape Evolution of Colloidal Nanocrystals. *Adv. Mater.* **2003**, *15*, 459.
2. Scher, E. C.; Manna, L.; Alivisatos, A. P. Shape Control and Applications of Nanocrystals. *Philos. Trans. R. Soc. London A* **2003**, *361*, 241.
3. Dick, K. A.; Deppert, K.; Larsson, M. W.; Martensson, T.; Seifert, W.; Wassenberg, L, R.; Samuelson, L. Synthesis of Branched 'Nanotrees' by Controlled Seeding of Multiple Branching Events. *Nat. Mater.* **2004**, *3*, 380.
4. Peng, Z. A.; Peng, X. Nearly Monodisperse and Shape-Controlled CdSe Nanocrystals via Alternative Routes: Nucleation and Growth. *J. Am. Chem. Soc.* **2002**, *124*, 3343.
5. Manna, L.; Milliron, D. J.; Meisel, A.; Scher, E. C.; Alivisatos, A. P. Controlled Growth of Tetrapod-branched Inorganic Nanocrystals. *Nat. Mater.* **2003**, *2*, 382.
6. Xie, R.; Kolb, U.; Bascche, T. Design and Synthesis of Colloidal Nanocrystal Heterostructures with Tetrapod Morphology. *Small* **2006**, *2*, 1454.
7. Burda, C.; Chen, X.; Narayanan, R.; El-Sayed, M. A. Chemistry and Properties of Nanocrystals of Different Shapes. *Chem. Rev.* **2005**, *105*, 1025.
8. Mokari, T.; Rothenberg, E.; Popov, I.; Costi, R.; Banin, U. Selective Growth of Metal Tips onto Semiconductor Quantum Rods and Tetrapods. *Science* **2004**, *304*, 1787.
9. Manna, L.; Scher, E. C.; Alivisatos, A. P. Synthesis of Soluble and Processable Rod-, Arrow-, Teardrop-, and Tetrapod-Shaped CdSe Nanocrystals. *J. Am. Chem. Soc.* **2000**, *122*, 12700.
10. Peng, X.; Manna, L.; Yang, W.; Wickham, J.; Sher, E.; Kadavanich, A.; Alivisatos, A. P. Shape Control of CdSe Nanocrystals. *Nature* **2000**, *404*, 59.
11. Yu, W. W.; Wang, Y. A.; Peng, X. Formation and Stability of Size-, Shape-, and Structure-Controlled CdTe Nanocrystals: Ligand Effects on Monomers and Nanocrystals. *Chem. Mater.* **2003**, *15*, 4300.
12. Langer, S. A.; Jackson, D. P.; Goldstein, R. E. Dynamics of Labyrinthine Pattern Formation in Magnetic Fluids. *Phys. Rev. A* **1992**, *46*, 4894.
13. Rosensweig, R. E.; Zahn, M.; Shumovich, R. Labyrinthine Instability in Magnetic and Electric Fuids. *J. Magn. Magn. Mater.* **1983**, *39*, 127.
14. Zahn, M.; Shumovich, R. Labyrinthine Instability in Dielectric Fluids. *IEEE Trans. Ind. Appl.* **1985**, *IA-21*, 53.
15. Elborai, S.; Kim, D. K.; He, X.; Lee, S. H.; Rhodes, S.; Zahn, M. Self-Forming, Quasi-Two-Dimensional Magnetic Fluid Patterns With Applied In-Phase-Rotating and DC-Axial Magnetic Fields. *J. Appl. Phys.* **2005**, *97*, 10Q3003.
16. Talapin, D. V.; Haubold, S.; Rogach, A. L.; Kornowski, A.; Haase, M.; Weller, H. A Novel Organometallic Synthesis of Highly Luminescent CdTe Nanocrystals. *J. Phys. Chem. B* **2001**, *105*, 2260.
17. Wuister, S. F.; Swart, I.; Driel, F. V; Hickey, S. G.; Donega, C. M. Highly Luminescent Water-Soluble CdTe Quantum Dots. *Nano Lett.* **2003**, *3*, 503.
18. Lunz, U.; Kuhn, J.; Goschenhofer, F.; Schussler, U.; Einfeldt, S.; Becker, C. R.; Landwehr, G. Temperature Dependence of the Energy Gap of Zinc-Blende CdSe and $Cd_{1-x}Zn_xSe$ Epitaxial Layers. *J. Appl. Phys.* **1996**, *80*, 6861.
19. Mei, J. R.; Lemos, V. Photoluminescence on CdSe and CdTe under Hydrostatic Pressure. *Solid State Commun.* **1984**, *52*, 785.
20. Li, Y.; Zhong, H.; Zhou, R. L.; Yang, C.; Yang, C.; Li, Y. High-Yield Fabrication and Electrochemical Characterization of Tetrapodal CdSe, CdTe, and CdSexTe1-*x* Nanocrystals. *Adv. Funct. Mater.* **2006**, *16*, 1705.

21. Granasy, L.; Pusztai, T.; Tegze, G.; Warren, J. A.; Douglas, J. F. On the Growth and Form of Spherulites. *Phys. Rev. E* **2005**, *72*, 011605.
22. Bailey, R.; Nie, S. Alloyed Semiconductor Quantum Dots: Tuning the Optical Properties without Changing the Particle Size. *J. Am. Chem. Soc* **2003**, *125*, 7100.
23. Manna, L.; Milliron, D. J.; Meisel, A.; Scher, E. C. Alivisatos, A. P. Controlled Growth of Tetrapod-Branched Inorganic Nanocrystals. *Nat. Mater.* **2003**, *2*, 382.
24. Milliron, D. J.; Hughes, S. M.; Cui, Y.; Manna, L.; Li, J. B.; Wang, L. W.; Alivisatos, A. P. Colloidal Nanocrystal Heterostructures with Linear and Branched Topology. *Nature* **2004**, *430*, 190.
25. Gudiksen, M.; Wang, J.; Lieber, C. Size Dependent Photoluminescence from Single Indium Phosphide Nanowires. *J. Phys. Chem. B* **2002**, *106*, 4036.
26. Li, L. S.; Hu, J. T.; Yang, W. D.; Alivisatos, A. P. Bandgap Variation of Size- and Shape-Controlled Colloidal CdSe Quantum Rods. *Nano Lett.* **2001**, *1*, 349.
27. Lee, W. Z.; Shu, G. W.; Wang, J. S.; Shen, J. L.; Lin, C. A.; Chang, W. H.; Ruaan, R. C.; Chou, W. C.; Lu, C. H.; Lee, Y. C. Recombination Dynamics of Luminescence in Colloidal CdSe/ZnS Quantum Dots. *Nanotechnology* **2005**, *16*, 1517.
28. Bawendi, P.; Carol, W.; Wilson, A.; Brus, L. Luminescence Properties of Cadmium Selenide Quantum Crystallites: Resonance Between Interior and Surface Localized States. *J. Chem. Phys.* **1992**, *96*, 946.
29. de Mello Donega, C.; Hickey, S. G.; Wuister, S. F.; Vanmaekelbergh, D.; Meijerink, A. Single Step Synthesis to Control the Photoluminescence Quantum Yield and Size Dispersion of CdSe Nanocrystals. *J. Phys. Chem. B* **2003**, *107*, 489.
30. Nirmal, M.; Norris, D.; Kumo, M.; Bawendi, M.; Efros, A.; Rosen, M. Observation of the 'Dark Exciton' in CdSe Quantum Dots. *Phys. Rev. Lett.* **1995**, *75*, 3728.
31. Ahmadi, T. S.; Wang, Z. L.; Green, T. C.; Henglein, A.; El-Sayed, M. A. Shape-Controlled Synthesis of Colloidal Platinum Nanoparticles. *Science* **1996**, *272*, 1924.
32. Puntes, V. F.; Krishnan, K. M.; Alivisatos, A. P. Colloidal Nanocrystal Size and Shape Control: the Case of Co. *Science* **2001**, *272*, 1924.
33. Dorsey, A. T.; Goldstein, R. E. The Shapes of Flux Domains in the Intermediate State of Type-I Superconductors. *Phys. Rev. B* **1998**, *57*, 3058.
34. Seul, M.; Andelman, D. Domain Shape and Patterns; the Phenomenology of Modulated Phases. *Science* **1995**, *267*, 476.
35. Shim, M.; Guyot-Sionnest, P. Optical Properties of Tetrapod-Shaped CdTe Nanocrystals. *Appl. Phys. Lett.* **2005**, *87*, 224101.
36. (a) Mullins, W. W.; Sekerka, R. F. Morphological Stability of a Particle Growing by Diffusion or Heat Flow. *J. Appl. Phys.* **1963**, *34*, 323. (b) Mullins, W. W.; Sekerka, R. F. Stability of a Planar Interface During Solidification of a Dilute Binary Alloy. *J. Appl. Phys.* **1964**, *35*, 444.
37. Ben-Jacob, E.; Garik, P. The Formation of Patterns in Non-Equilibrium Growth. *Nature* **1990**, *343*, 523.
38. Safffman, P. G.; Taylor, G. I. The Penetration of a Fluid into a Porous Medium or Hele-Shaw Cell Containing a More Viscous Liquid. *Proc. R. Soc. A* **1958**, *245*, 312.
39. Mandelbrot, B. B. *The Fractal Geometry of Nature*; W. H. Freeman and Co.: San Francisco, 1982.
40. Petrich, D. M.; Goldstein, R. E. Nonlocal Contour Dynamics Model for Chemical Front Motion. *Phys. Rev. Lett.* **1994**, *72*, 1120.
41. Goldstein, R. E.; Muraki, D. J.; Petrich, D. M. Interface Proliferation and the Growth of Labyrinths in a Reaction-Diffusion System. *Phys. Rev. E* **1996**, *53*, 3933.
42. Rosensweig, R. E. *Ferrohydrodynamics*; Cambridge University Press: Cambridge, 1985.
43. Portmann, O.; Vaterlaus, A.; Pescia, D. An Inverse Transition of Magnetic Domain Patterns in Ultrathin Films. *Nature* **2003**, *422*, 701. Benkowski, J. J.; Jones, R. L.; Douglas, J. F.; Karim, A. Photocurable Oil/Water Interface as a Universal Platform for 2-D Self-Assembly. *Langmuir* **2007**, *22*, 3530.
44. Goldstein, R. E.; Jackson, D. P.; Dorsey, A. T. Interacting Current Loop Model for the Intermediate State in Type-I Superconductors. *Phys. Rev. Lett.* **1996**, *76*, 3818.
45. Stine, K. J.; Bono, M. F.; Kretzer, J. S. Observation of a Foam Morphology of the Liquid-Condensed Phase of a Langmuir Monolayer. *J. Colloid Interface Sci.* **1994**, *162*, 320.
46. Toxvaerd, S. Molecular Dynamics Simulation of Domain Formation in Langmuir Monolayers of Molecules with Dipole Moments. *Mol. Phys.* **1998**, *95*, 539.
47. Reimann, B.; Richter, R.; Rehberg, I. Glasslike Relaxation of Labyrinthine Domain Pattern. *Phys. Rev. E* **2002**, *65*, 031504.
48. Miura, S.; Mino, M.; Yamazaki, H. Relaxation of Labyrinth Domain Structure of Ferromagnetic Thin Film under Field Cycles. *J. Phys. Soc. Jpn.* **2001**, *70*, 2821.
49. Garfinkel, A.; Tintut, Y.; Petrasek, D.; Bostro, K.; Demer, L. L. Pattern Formation by Vascular Mesenchymal Cells. *Proc. Natl. Acad. Sci. U.S.A.* **2004**, *101*, 9247.
50. Hasen, J.; Pfeiffer, L. N.; Pinczuk, A.; He, S.; West, K. W.; Dennis, B. S. Metamorphosis of a Quantum Wire into Quantum Dots. *Nature (London)* **1997**, *390*, 54.
51. Granasy, L.; Pusztai, L.; Borzsonyi, T.; Warren, A.; Douglas, J. F. A General Mechanism of Polycrystalline Growth. *Nat. Mater.* **2004**, *3*, 645.
52. Hu, J.; Li, L.; Yang, W.; Manna, L.; Wang, L.; Alivisatos, A. P. Linearly Polarized Emission from Colloidal Semiconductor Quantum Rods. *Science* **2001**, *292*, 2060.
53. Lin, Y.; Hsieh, M.; Liu, C.; Chang, H. T. Photoassisted Synthesis of CdSe and Core-Shell CdSe/CdS Quantum Dots. *Langmuir* **2005**, *21*, 728.
54. Cullis, A. G.; Canhan, L. T. Visible Light Emission Due to Quantum Size Effects in Highly Porous Crystalline Silicon. *Nature* **1991**, *353*, 335.
55. Goñi, A. R.; Pfeiffer, L. N.; West, K.; Pinzuck, A.; Baranger, H. U.; Stormer, H. L. Observation of Quantum Wire Formation At Intersecting Quantum Wells. *Appl. Phys. Lett.* **1992**, *61*, 1956.
56. Someya, T.; Akiyama, H.; Sakaki, H. Tightly Confined One-Dimensional States in T-Shaped GaAs Edge Quantum Wires with AlAs Barriers. *Appl. Phys. Lett.* **1995**, *66*, 3672.
57. Gislason, H.; Langbein, W.; Hvam, J. M. Asymmetric GaAs/AlGaAs T-Wires with Large Confinement Energies. *Appl. Phys. Lett.* **1996**, *69*, 3248.
58. Sapoval, B.; Russ, S.; Chazalviel, J. A. Eigenstates in Irregular Quantum Wells: Application to Porous Silicon. *J. Phys.: Condens. Matter.* **1996**, *8*, 6235.
59. Sapoval, B.; Gobron, T. Vibrations of Strongly Irregular or Fractal Resonators. *Phys. Rev. E* **1993**, *47*, 3013.
60. Even, C.; Russ, S.; Rapin, V.; Piranski, P.; Sapoval, B. Localizations in Fractal Drums: An Experimental Study. *Phys. Rev. Lett.* **1999**, *83*, 726.
61. Sapoval, B.; Russ, S. Effect of Geometrical Irregularities on the Band Gap of Porous Silicon. *Mater. Res. Symp. Proc.* **1995**, *358*, 37.
62. Brus, L. Electron–Electron and Electron–Hole Interactions in Small Semiconductor Crystallites: the Size Dependence of the Lowest Excited Electronic State. *J. Chem. Phys.* **1984**, *80*, 4403.
63. Salman, A. A.; Tortschanoff, A.; Mohamed, M. B.; Tonti, D.; van Mourik, F.; Chergui, M. Temperature Effects on the Spectral Properties of Colloidal CdSe Nanodots, Nanorods, and Tetrapods. *Appl. Phys. Lett.* **2007**, *90*, 93104.
64. Pang, Q.; Zhao, L.; Cai, Y.; Nguyen, D. P.; Regnault, N.; Wang, N.; Yang, S.; Weikun, G.; Ferreira, R.; Bastard, G.; Wang, J. CdSe Nano-tetrapods: Controllable Synthesis, Structure Analysis, and Electronic and Optical Properties. *J. Chem. Mater.* **2005**, *17*, 5263–5267.
65. Li, J.; Wang, L. W. Shape Effects on Electronic States of Nanocrystals. *Nano Lett.* **2003**, *3*, 1357.
66. Tari, D.; De Giorgi, M.; Della Sala, F.; Carbone, L.; Krahne, R.; Manna, L.; Cingolani, R.; Kudera, S.; Parak, W. J. Optical Properties of Tetrapod-Shaped CdTe Nanocrystals. *Appl. Phys. Lett.* **2005**, *87*, 224101.

67. Tang, Z.; Kotov, N. A.; Giersig, M. Spontaneous Organization of Single CdTe Nanoparticles into Luminescent Nanowires. *Science* **2002**, *297*, 237.
68. Zhang, X.; Zhang, Z.; Han, X. Synthesis of Coral-Like Nickel Nanocrystallites via a Dipolar-Interaction-Directed Self-Assembly Process. *J. Cryst. Growth* **2005**, *274*, 113.
69. Sawada, S.; Hamada, N.; Ookubo, N. Mechanisms of Visible Photoluminescence in Porous Silicon. *Phys. Rev. B* **1994**, *49*, 5236.
70. Yu, Y.; Han, S.; Chu, X.; Chu, S.; Wang, Z. Coherent Temporal Oscillations of Macroscopic Quantum States in a Josephson Junction. *Science* **2002**, *296*, 889.
71. (a) Elder, A. D.; Mathew, S. M.; Swarthy, J.; Yunus, K.; Frank, J. H.; Brennan, C. M.; Fisher, A. C.; Kaminski, C. F. Application of Frequency-Domain Fluorescence Lifetime Imaging Microscopy as a Quantitative Analytical Tool for Microfluidic Devices. *Opt. Express* **2006**, *14*, 5456. (b) Magde, D.; Wong, R.; Seybold, P. G. Fluorescence Quantum Yields and Their Relation to Lifetimes of Rhodamine 6G and Fluorescein in Nine Solvents: Improved Absolute Standards for Quantum Yields. *Photochem. Photobiol* **2002**, *75*, 327. (c) Magde, D.; Rojas, G. E.; Seybold, P. G. Solvent Dependence of the Fluorescence Lifetimes of Xanthene Dyes. *Photochem. Photobiol.* **1999**, *70*, 737.
72. Identification of a commercial product is made only to facilitate reproducibility and to adequately describe procedure. In no case does it imply endorsement by NIST or imply that it is necessarily the best product for the procedure.